



Efficiency investigations of electrochemical realkalisation treatment applied to carbonated reinforced concrete – Part 1: Sacrificial anode process

YunYun Tong^a, Véronique Bouteiller^{a,*}, Elisabeth Marie-Victoire^b, Suzanne Joiret^c

^a Université Paris Est, IFSTTAR, SOA, F-75732, Paris, France

^b Laboratoire de Recherche des Monuments Historiques, 29, rue de Paris, 77420 Champs sur Marne, France

^c Laboratoire Interfaces et Systèmes Electrochimiques, UPR 15, CNRS, Université P. et M. Curie, 4, place Jussieu, 75252 Paris Cedex 05, France

ARTICLE INFO

Article history:

Received 23 September 2010

Accepted 17 August 2011

Keywords:

pH (A)

Carbonation (B)

Electrochemical properties (C)

Reinforcement (D)

Concrete (E)

ABSTRACT

The aim of this study was to assess the efficiency of a realkalisation treatment using sacrificial anodes applied to reinforced concrete degraded by carbonation. Analytical determinations (acid/base indicators, quantitative pH, alkaline profiles, SEM and micro-Raman) together with electrochemical characterizations (rest potential, impedance, linear polarisation resistance and corrosion current densities) were performed on artificially carbonated slabs, before and after treatment (mainly 15 days, 11 weeks, 6 and 12 months). The treatment efficiency was demonstrated by an increase of pH and by an alkaline ion penetration in the concrete cover. Rest potential and corrosion current densities indicated a slight decrease of the rebar corrosion activity. Complementary Raman spectroscopy showed a change in the oxide species and SEM observations indicated that the cement matrix remained almost unchanged.

© 2011 Elsevier Ltd. All rights reserved.

1. Introduction

Carbonation induced corrosion is a major cause of decay of reinforced concrete structures in the fields of buildings, civil engineering bridges or historical monuments. As long as the rebars are in a high alkalinity environment concrete, they remain passive. The natural ageing carbonation process leads to a consumption of portlandite inducing a decrease of the pH of the concrete cover which is then no longer protective and an active corrosion of rebars can take place [1–3].

A precise overview of possible actions for the protection and repair of concrete structures is presented in the EN 1504 European standard [4]. Usually, in France, when carbonation is implicated, degraded reinforced concrete structures are repaired using the “patch” technique. However this kind of repair is not entirely satisfactory because of the “incipient anode effect”. Thus when a patch repair, with a very high pH, is placed side by side with a carbonated area, an anode effect can induce the corrosion of the rebars covered with the carbonated concrete [5]. In the 1980s, electrochemical realkalisation treatment was developed to repair reinforced concrete structures affected by carbonation [6]. In 1994, Pocock [7] presented an overview of electrochemical techniques as alternative repair options. In 1998, Mietz [8] presented a state of the art report on these electrochemical rehabilitation methods for reinforced concrete structures. These techniques consist in using the concrete rebars as a cathode, to temporarily

apply an anode on the concrete surface (Fig. 1), and to generate a current between both electrodes. Electrical conductivity is assessed by an alkaline electrolyte contained in a cellulose pad. Current can be supplied by an external electrical power source (impressed current (IC) process) or by using specific anodes composed of a metal less noble than the rebars (sacrificial anode (SA) process).

Realkalisation based on impressed current process either in laboratory experiments [8–21], or in the field [22,23], is well documented. Moreover, the European specification CEN/TS 14038–1 [24] indicates that the termination of the treatment is achieved when a total charge of 200 A.h/m² has been delivered; and that the effectiveness of the realkalisation can be evaluated by phenolphthalein pH test (pink coloration around the rebar to a minimum of 10 mm or the bar diameter).

During the electrochemical realkalisation by impressed current (Fig. 1), according to Mietz, [9], the following mechanisms take place:

- absorption due to capillary effects of dissociated alkaline solution
- diffusion of alkaline compounds due to the difference in concentrations
- migration of ions within the electrical field (negative ions move towards the anode (e.g. OH[−], Cl[−] ions), and positive ions move towards the cathode (e.g. Na⁺ or K⁺ ions)).
- electrolysis at the electrodes. Around the cathode (rebar), hydroxyl ions are generated (2H₂O + 2e[−] = H₂ + 2OH[−]). In addition, reaction with oxygen diffused into the concrete takes place (½O₂ + H₂O + 2e[−] = 2OH[−]). At the anode, oxidations occurs (2OH[−] = ½O₂ + H₂O + 2e[−]).
- electro osmosis: the electrolyte at the concrete surface moves toward the cathode due to the electrical field.

* Corresponding author at: IFSTTAR, SDO, 58 Boulevard Lefebvre 75732 Paris Cedex 15, France. Tel.: +33 140435113; fax: +33 140436598.

E-mail address: veronique.bouteiller@ifsttar.fr (V. Bouteiller).

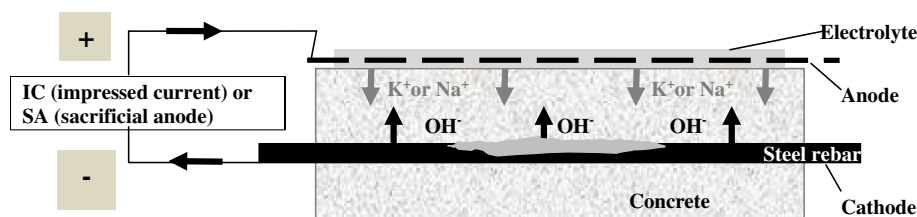


Fig. 1. Realkalisation mechanisms.

The alkaline solution (commonly sodium or potassium carbonate) migrates into the carbonated concrete while hydroxyl ions are simultaneously produced by water electrolysis around the rebars, both phenomena being expected to raise the pH and re-establish the passive layer.

Realkalisation based on sacrificial anode process is only stated in a few congress proceedings [21], [25–27]. In this process, there is no electrical power source. Electrons are supplied by the oxidation of an anode made of a less noble metal than steel. This process introduced metallic cations from the anode in the system. However, the galvanic current can only be measured and the duration of the treatment is not known in advance.

The aim of this paper was to check the efficiency and the durability of a realkalisation treatment using sacrificial anodes. Some questions were more specifically addressed:

As the galvanic current intensity is smaller compared to that provided by the impressed current process, will it contribute to a sufficient increase of pH (considering a total charge of about 200 A.h/m² of steel)?

As for the same total charge, SA duration treatment is longer than that of IC-process, what will be the alkaline ion concentration at the steel level after treatment?

Finally, two more general questions (valid for IC as well as AS processes) were:

How to ascertain not only the concrete realkalisation, but also the steel passivity?

How long is the treatment effective?

To answer those questions, firstly, an experimental study on electrochemical realkalisation treatment using sacrificial anodes applied to carbonated concrete slabs [28] (concrete was chosen because more representative of real structures than steel in solutions or steel embedded in mortars) was realised. Secondly, an investigation on the treatment efficiency both on concrete and on the corrosion conditions of steel reinforcement was performed. Concerning the effect on concrete, classical analytical characterizations such as colour indicators tests, and alkaline concentration evaluations were performed. Quantitative pH measurements were also conducted. Concerning the corrosion conditions of steel reinforcement, a complete set of electrochemical characterizations was performed using not only half-cell potential (the most widely used technique), but also linear polarisation resistance and impedance measurements, in order to calculate corrosion current densities. Moreover, Raman Micro-spectroscopy identifications and SEM observations helped in the rust and in the steel/concrete interface examinations. Finally, treatment efficiency was investigated in a 12 month study.

2. Experimental

2.1. Specimens

Seven reinforced concrete slabs (dimensions 300×300×50 mm, weight≈12 kg) were cast using Portland cement (CEM I, 275 kg/m³) and a 0.7 water to cement ratio (according to the EN 1766 Standard). The mix proportions are indicated in Table 1. The Palvadeau aggregates are considered none alkali-reactive. The reinforcement consisted in three parallel steel rebars (6 mm in diameter and 400 mm in length)

with a concrete cover of 22 mm. On these rebars, a 100 mm zone on each end was coated with an epoxy cataphoretic paint, to delimitate a 200 mm steel studied zone in the centre (Fig. 2).

After a 28 day cure in water, one slab was kept as a sound concrete reference (1-S) and the other six were submitted to an artificial accelerated carbonation [29] (pre-conditioning 1 month at 45 °C and 60% RH and then carbonation for a period of 2 months at 22 °C, 50% CO₂ and 60% RH). After carbonation, two slabs were kept as carbonated references (2-C and 3-C) and the other four slabs were treated by realkalisation using sacrificial anodes (8-SA, 9-SA, 10-SA and 11-SA). All the slabs were stored in the laboratory (20 °C ± 2 °C, 60% RH ± 10% RH) both before and after the realkalisation treatment.

2.2. Realkalisation treatment using sacrificial anodes

Four slabs (08, 09, 10 and 11-SA) were realkalised by a specialised Company. The anode, a 5×5 mm mesh grid, 2 mm in diameter, made of an aluminium alloy was directly connected to the three rebars. A sodium carbonate-based electrolyte was used to wet a cellulose pad which was applied on the top surface of the slabs. The cellulose pad was kept wet by spraying water on a daily basis.

2.3. Treatment efficiency evaluations

2.3.1. Analytical characterizations

Analytical characterizations were performed in order to both evaluate the alkalinity evolution of the concrete cover after realkalisation and to detect potential side effects such as deleterious transformations of the cement matrix. Sampling locations of analytical characterizations are presented in Fig. 3.

To highlight the realkalised zones, two colour indicators were used: phenolphthalein and thymolphthalein which respectively turn to pink and blue, when the pH is above 10 and 11 (both indicators appear colourless for lower pH values). They were sprayed on freshly sawn slab surfaces.

For quantitative pH determination and sodium analysis, cores were drilled and cut into five 10 mm thick slices, which were dried in an oven at 45 °C for 1 week, before being grounded into a 315 μm powder and stored in small plastic containers (to prevent further carbonation). The pH was then determined according to the procedure described by Räsänen [30], while sodium was titrated using atomic absorption spectroscopy.

The steel–concrete interface was analysed with a Jobin-Yvon Horida (LABRAM) Raman spectrometer, consisting of an Olympus BX40 microscope confocally coupled to a 300 mm focal length spectrograph, equipped with an holographic grating (1800 grooves.mm^{−1}) and a

Table 1
Mix design of the concrete slabs (kg/m³).

Cement CEM I 42.5 R	Palvadeau aggregates (non reactive)										Water
275	0/0.315	0.315/1	0.5/1	1/4	2/4	4/8	8/12	12.5/16	192.50		
149	277	180	170	57	324	265	473				

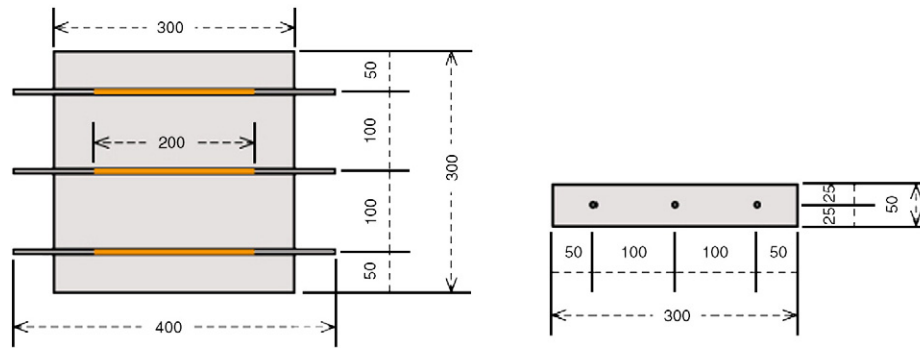


Fig. 2. Design of the reinforced concrete slabs (dimensions in mm).

Peltier cooled CCD detector (1024×256 pixels). The spectra were obtained with 632 nm radiation from an internal 10 mW HeNe laser with neutral density filters to avoid any thermal effect as iron III compounds can be modified under laser irradiation. For measurements, a *100 ULWD objective was used to focus laser light and collect spectra, giving a lateral resolution of 2 μ m. Samples were analysed either on a cross section or on the lateral surface of the rebar after concrete fracture.

In order to highlight any cement matrix transformation, and to examine the steel/concrete interface, fractured samples were observed with a Scanning Electron Microscope combined with an Energy Dispersive Spectrometer (JEOL JSM-5600 + Oxford Link-PentaJet-6587 EDS).

2.3.2. Electrochemical measurements

To evaluate the evolution of the steel rebar corrosion before and after realkalisation, electrochemical measurements were performed. As such measurements are highly dependent upon temperature and humidity, the slabs were immersed in water 24 h prior to the measurements that were performed in the laboratory.

The electrochemical system was composed of three electrodes: the working electrode was the steel rebars, the reference electrode was a KCl saturated calomel electrode (SCE) (E vs NHE = +242 mV) and the counter electrode was a titanium/platinum-based grid, the chosen electrolyte being tap water.

The measurements were conducted on 9 electrochemical cells (3 cells per rebar) for each slab, with a portable potentiostat PARSTAT PAR2263 [31], as illustrated in Fig. 4.

As an example, Fig. 5 illustrates the electrochemical characterizations of slab 10-SA, rebar 3, cell 8, 6 months after treatment with

the records of open circuit potential (Fig. 5a), Nyquist diagram (Fig. 5b) and linear polarisation resistance (Fig. 5c).

The rest potential, E_{corr} (mV), was determined from the potential versus time curve (Fig. 5a), after 10 min (the potential having reached its equilibrium). The impedance technique (frequency range from 100 kHz to 39 mHz) was used to determine both the concrete cover and the electrolyte resistance, R_e (Ohm), from the Nyquist diagram (Fig. 5b). The R_e value was taken as the real part of the impedance corresponding to the lowest point of the imaginary part of the impedance. Using the linear polarisation technique [32,33], (± 10 mV around the rest potential using a sweep rate of 2.5 mV/min), the current versus the voltage was recorded (Fig. 5c, grey hysteresis). For the values of the hysteresis in between 0 and +10 mV around E_{corr} , (Fig. 5c, black points), the inverse of the slope of the current versus voltage curve ($1/\text{slope} = R_e + R_p$), was determined. The polarisation resistance of the steel rebar, R_p (Ohm), was then calculated.

The corrosion current density, I_{corr} ($\mu\text{A}/\text{cm}^2$), (taking into account the ohmic drop and the polarised surface), was finally calculated based on the Stern and Geary Eq. (1).

$$I_{\text{corr}} = B/(R_p \cdot S) \quad (1)$$

with B a constant (26 mV), R_p (ohm) the polarisation resistance and S (cm^2) the polarised steel surface corresponding to the electrochemical cell design (10.2 cm^2 in this case).

In this paper, the electrochemical results are expressed per slab considering the average of the nine cells. Table 2 gives the results for slab 10-SA, 6 months after treatment as an example.

The reproducibility and repeatability of the electrochemical measurements studied in details in [28] showed that the immersion of the slab prior to measurements is essential to obtain reproducible data and that the results monitored on a day time are repeatable because the slab moisture content remained constant (considering cells 3, 8 and 5 and three repeated measurements per cell on the same day).

3. Results

3.1. Realkalisation treatment using sacrificial anode monitoring

Fig. 6a presents the realkalisation set up. At the end of the treatment (33 days), the anodes were almost completely consumed (Fig. 6b). In order to calculate the total electrical charge, the galvanic current was measured during the treatment using a 1 ohm resistance. It varied from 0.40 mA/m² of steel up to 1.86 mA/m² of steel and ended close to 0 (Fig. 7). The treatment was stopped after 33 days because the anode was consumed. By then, the total charge was equal or higher than 200 A.h/m² [24] of steel (202, 226, 269 and 269 A.h/m² steel respectively for slabs 08, 09, 10 and 11-SA). The evolution of the cathodic potentials during the treatment (Fig. 8) showed that the three rebars of each slab reacted similarly. Moreover, the

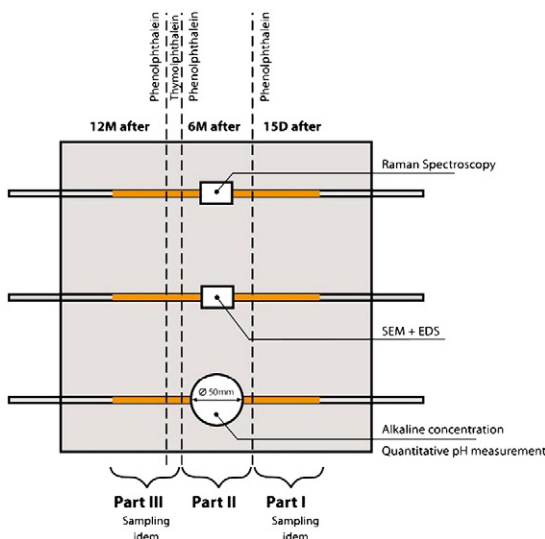


Fig. 3. Sampling locations of analytical characterizations.

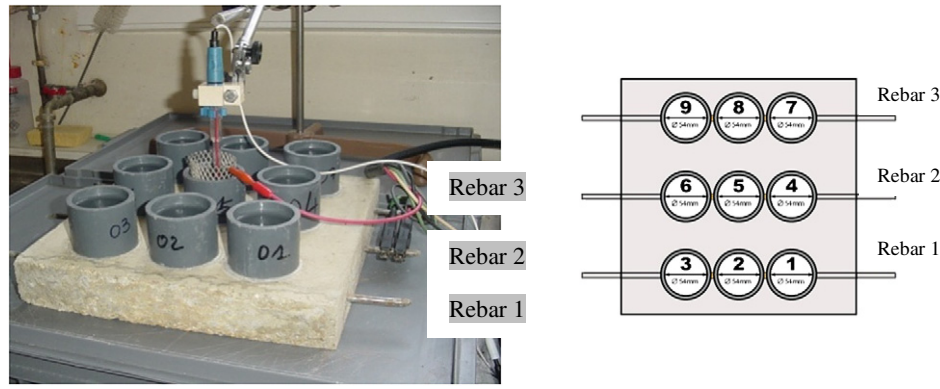


Fig. 4. Electrochemical system (9 cells per slab).

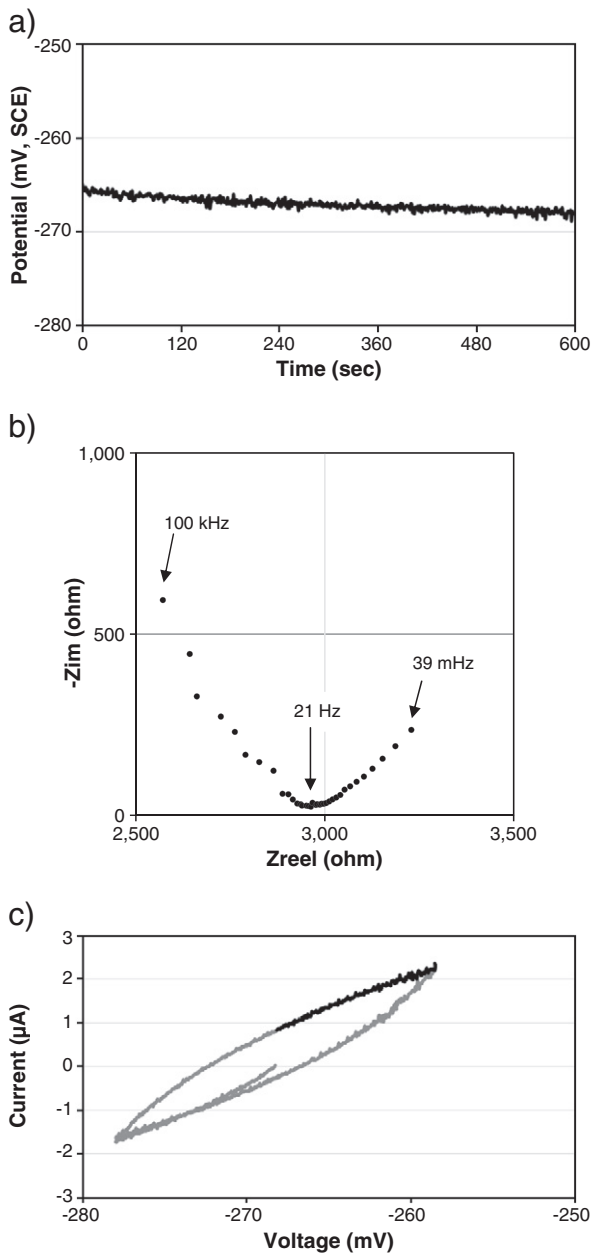


Fig. 5. Example of electrochemical measurements on slab 10-SA, 6 months after treatment (rebar 3, cell 8), a) Rest potential, b) Nyquist diagram, and c) Linear polarisation resistance.

behaviour of the four slabs was almost the same (data not shown). For almost the first three weeks, the cathodic potentials remained in the range -1.6 to -1.8 V vs. SCE and then they became progressively more positive. At the end of the treatment, the mean cathodic potential values (average of the three rebars) were respectively equal to -0.914 , -0.651 , -0.755 and -0.679 V vs. SCE for slabs 08, 09, 10 and 11-SA. After treatment, in order to wait for the rebars depolarisation, the electrochemical measurements were performed 15 days after the end of the treatment (although that according to the potential measurements (data not shown), 3 days were enough to obtain the depolarisation).

3.2. Treatment efficiency investigations

3.2.1. Evolution of the concrete alkalinity

3.2.1.1. Colour indicator qualitative tests. The results of the phenolphthalein and thymolphthalein tests, before and after realkalisation treatment, are illustrated in Fig. 9.

Concerning the carbonated concrete reference (slab 3-C), after spraying, the two colour indicators remained colourless, indicating a complete carbonation of the 5 cm concrete thickness as expected after the artificial accelerated carbonation.

On the 11-SA treated slab, 15 days after treatment, a realkalisation of the concrete from the treated surface to the rebars was revealed using the phenolphthalein test (pink). Six months after treatment, the same realkalised areas were highlighted with the phenolphthalein test, and a complementary thymolphthalein test was performed indicating that the pH of the concrete around the rebars was higher than 11 (blue).

These results clearly showed the efficiency of realkalisation treatment using sacrificial anodes. However, as the pink colour observed

Table 2
Electrochemical characterizations of slab 10-SA, 6 months after treatment.

		Ecorr mV, SCE)	Re (ohm)	1/slope (ohm)	R ²	Rp (ohm)	Surface (cm ²)	icorr (µA/cm ²)
Rebar 1	Cell 1	−237	2147	6410	0.99	4263	10.2	0.6
	Cell 2	−230	1967	6849	0.99	4882	10.2	0.5
	Cell 3	−223	2218	6623	0.99	4405	10.2	0.6
Rebar 2	Cell 4	−298	1953	4329	0.99	2376	10.2	1.1
	Cell 5	−283	1509	3953	0.99	2444	10.2	1.0
	Cell 6	−284	2077	4902	0.99	2825	10.2	0.9
Rebar 3	Cell 7	−304	2976	6536	0.99	3560	10.2	0.7
	Cell 8	−268	2958	6944	0.99	3986	10.2	0.6
	Cell 9	−322	3409	6289	0.99	2880	10.2	0.9
Slab	Average	−272	2357	5871		3513		0.8
	Deviation	35	615	1150		920		0.2

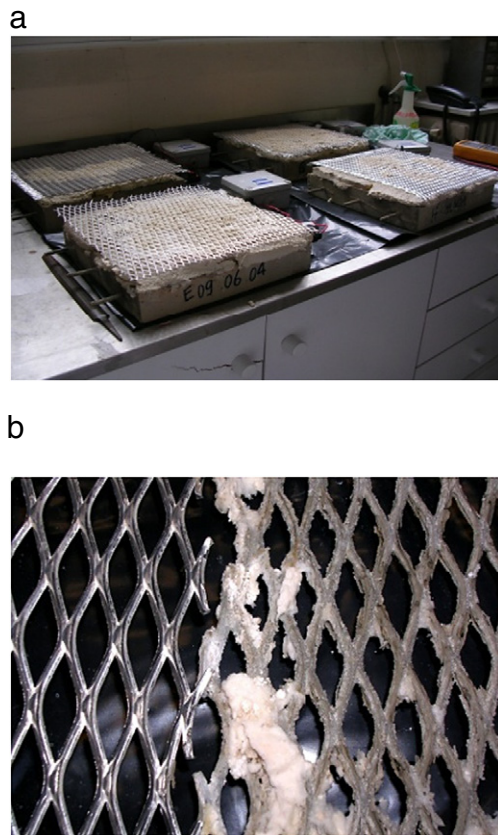


Fig. 6. Realkalisation treatment using sacrificial anodes. a) Realkalisation treatment application. b) Aluminium alloy anode before treatment (left) and consumed anode (right) at the end of treatment.

after the phenolphthalein spraying was less and less obvious on the tests performed 6 months and 12 months after treatment, the durability of this efficiency was questionable.

Thus, complementary pH measurements were performed to quantify the concrete realkalisation and its evolution in time.

3.2.1.2. Quantitative pH measurements. Quantitative pH measurements were performed by the mean of mixing concrete powder with a solvent as developed by Räsänen [30]. This method allows the determination of the pH of concretes while pore water extraction using high pressure is only possible for pastes or mortars [34]. Moreover, Räsänen's technique needs a relatively short experimentation time (15 min) compared to other techniques such as in-situ leaching technique [35] (8 weeks conditioning) or ex-situ leaching techniques [36] (minimum of 3 days leaching). Fig. 10 presents the quantitative pH profile determinations of the 11-SA treated slab, 6 and 12 months after treatment together

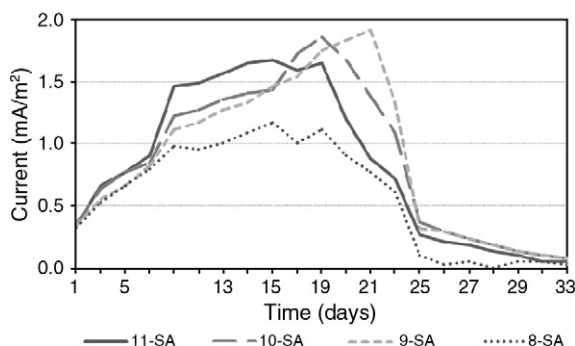


Fig. 7. Galvanic currents during treatment for the four treated slabs.

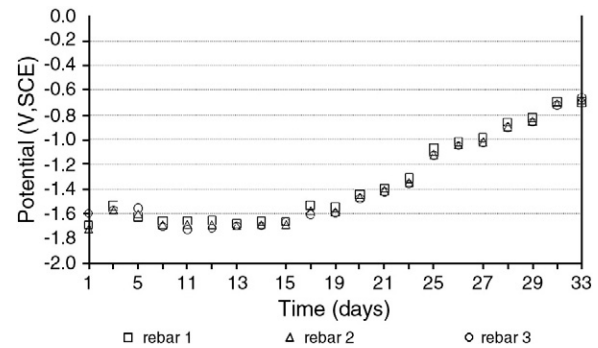


Fig. 8. Evolution of the cathodic potentials during treatment (example of slab 11-SA).

with those of the sound concrete reference (1-S, pH = 12.5) and of the carbonated concrete reference found in this study (12.5) can be somehow different from those obtained by Longuet [34] (13 or higher), Li [36] (13.52) or Sagues [35] (12.82), but is rather in good agreement with the value found by Räsänen (12.64). This difference can probably be explained by the type of cement and also by the operating mode.

Six months after treatment, the concrete around the rebars was clearly realkalised (pH = 11.7 at a depth of 20–30 mm) as well as the top concrete surface where the treatment had been applied (pH = 10.7 at 0–10 mm). Twelve months after treatment, the pH value of the concrete around the rebars decreased to a 10.8 pH value whereas the pH of the top concrete surface remained unchanged.

It is to be noticed that the pH of the bottom surface of the slab (depth 40–50 mm) was equal to 10.4 after treatment. However, this pH increase cannot be attributed to the realkalisation treatment as there was no electrical field between the rebar and the bottom of the slab. This result can probably be explained by the capillary absorption of the alkaline electrolyte, which ran down the slab during the treatment, into the concrete cover.

These quantitative results showed that the realkalisation treatment yields an increase of the pH compared to the carbonated concrete reference slab (3-C). Even if the absolute value can depend on the operating mode, the difference of pH between the sound concrete and the realkalised one is pertinent. Yet, the pH of the sound concrete was not recovered.

3.2.1.3. Alkaline concentration profiles. The sodium concentration profiles obtained on slab 11-SA, 6 months and 12 months after treatment, are illustrated in Fig. 11 together with the average sodium concentration (0.03%) measured on the carbonated concrete reference slab (3-C).

Six months after the realkalisation (that lasted 33 days), a great increase of sodium ion concentration was detected compared to that of the carbonated control: 0.47% (21 times higher) on the treated surface, 0.11% (5 times higher) at the rebar level and 0.23% (10 times higher) at the bottom surface. Twelve months after treatment, the sodium concentration profiles remained almost unchanged.

During the realkalisation treatment, the sodium ions contained in the electrolyte are supposed to penetrate into the concrete according to three main processes: electrical migration, capillary absorption and gravity. From these results, although the contribution of each of the three transport processes cannot be clearly distinguished, the capillary contribution was evidenced by the sodium concentration increase observed on the bottom of the slab (depth 30 to 50 mm) where electrical migration and gravity effects were absent.

3.2.2. Evolution of the corrosion activity of the steel rebars

3.2.2.1. Rest potential. The rest potential measured on the three treated slabs (8, 9 and 10-SA) before and after (15 days, 11 weeks, 6 months and 12 months) the realkalisation treatment, together with the evolution

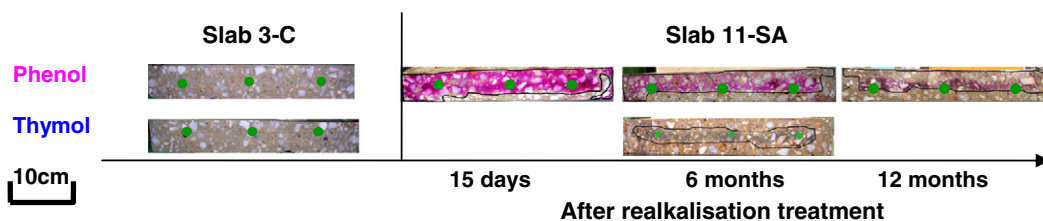


Fig. 9. Phenolphthalein and thymolphthalein test results.

of the rest potentials of the sound (1-S) and the carbonated (2-C) concrete reference slabs are presented in Fig. 12. In this figure, the dotted lines represent the ASTM C876 corrosion probabilities [37], which are below 10% when the rest potential is more positive than -120 mV vs. SCE and above 90% when the rest potential is more negative than -276 mV vs. SCE.

For the sound concrete reference slab (1-S), the rest potential values versus time were always higher than -200 mV and the probability of corrosion can be considered as uncertain. The rebars remained passive.

For the four carbonated concrete slabs (3, 8, 9 and 10), before treatment, the rest potential values ranged from -320 to -450 mV and were therefore indicative of a high probability of corrosion. In time, the carbonated concrete reference slab 2-C always showed rest potential values below -400 mV whereas, for the realkalised slabs (8, 9 and 10-SA), the rest potentials increased with time (shift of 100 mV 6 months after treatment, except for slab 9 which had the highest initial rest potential). Twelve months after treatment, the rest potentials measured on the treated slabs compared to their initial values (before treatment) and the carbonated reference values (on the same time scale) remained more positive.

This increase of the rest potentials observed on the treated slabs is consistent with a decrease of the corrosion activity up to a year after realkalisation. Nevertheless, if potential values are indicative of a propensity to corrosion, they don't give any information on the corrosion rate. Thus, in order to calculate a corrosion current density, linear polarisation resistance and impedance measurements were performed.

3.2.2.2. Corrosion current density. Corrosion current density obtained on the three treated slabs (8, 9 and 10-SA) before and after (15 days, 11 weeks, 6 months and 12 months) the realkalisation treatment, together with the corrosion current density evolution of the sound (1-S) and the carbonated (2-C) concrete reference slabs are presented in Fig. 13. In this figure, the dotted lines represent the four ranges of corrosion levels based on RILEM studies [38]: below $0.1 \mu\text{A}/\text{cm}^2$, the level of corrosion is negligible; from 0.1 to $0.5 \mu\text{A}/\text{cm}^2$, corrosion is weak; from 0.5 to $1 \mu\text{A}/\text{cm}^2$, corrosion is moderate and for values higher than $1 \mu\text{A}/\text{cm}^2$, corrosion is high.

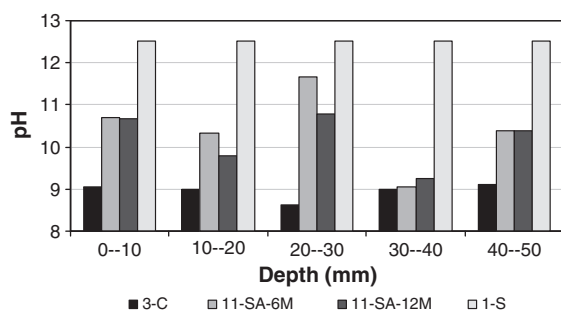


Fig. 10. pH profiles for references and treated slabs, 6 and 12 months after treatment (rebar depth is 25 mm).

For the sound concrete reference (1-S), the assessed corrosion current densities were close to $0.1 \mu\text{A}/\text{cm}^2$, whatever the time, indicating a negligible corrosion activity, whereas for the carbonated concrete reference (2-C), the corrosion current densities remained higher than $1.5 \mu\text{A}/\text{cm}^2$ indicating a high corrosion activity.

Before treatment, for slabs 8, 9 and 10-SA, the corrosion current densities were ranging from 1 to $1.8 \mu\text{A}/\text{cm}^2$, when on the same slabs after the realkalisation treatment, the corrosion current densities decreased with time, down to values close to $0.7 \mu\text{A}/\text{cm}^2$ twelve months after treatment, with a change of corrosion activity range from high to moderate. Nevertheless, the negligible corrosion level of the rebars observed in the sound concrete was not reached.

Therefore, the decrease of the corrosion current densities observed after the realkalisation treatment was consistent with a slowdown of the corrosion activity, but not with a re-passivation.

3.2.3. Corrosion products and cement matrix evolution

3.2.3.1. Corrosion product identification using Raman spectroscopy. Due to the presence of fluorescent compounds in concrete, Raman spectra recorded in this study present a high fluorescent background. It was removed for all the spectra given here for the sake of clarity, except for the first of them.

The Raman spectrum of non carbonated concrete indicated pure magnetite, Fe_3O_4 , (Fig. 14), characterised by a strong band at 670 cm^{-1} , recorded regardless of the place analysed along the rebar. Magnetite has also been observed by Marcotte [39]. From optical observations, this layer was homogeneous, adherent to the rebar and presented a thickness below $2 \mu\text{m}$ after 30 months.

Raman analysis on the corrosion layers of the rebars embedded in carbonated or treated concrete gave the same results: the corrosion layer was adhesive on both sides (concrete or rebar) with a thickness of around $20 \mu\text{m}$ but inhomogeneous. This can be seen in the optical picture given in Fig. 15.

A thin, black layer with veins inside the corrosion layer was observed at the metal interface, the Raman spectrum associated to this layer is the one of magnetite already given in Fig. 14 or the Raman spectrum of Fig. 16, which is a mixture of hematite and magnetite whatever the laser intensity used. The presence of hematite ($\alpha\text{-Fe}_2\text{O}_3$) with

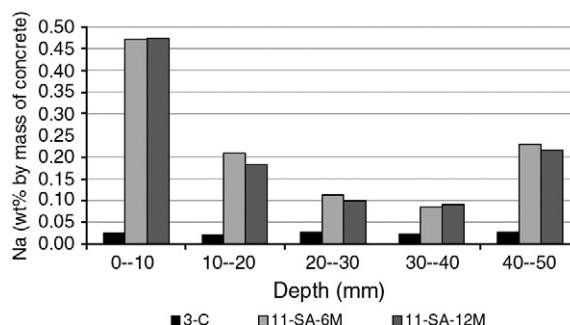


Fig. 11. Sodium concentration profiles for references and treated slabs, 6 and 12 months after treatment (rebar depth is 25 mm).

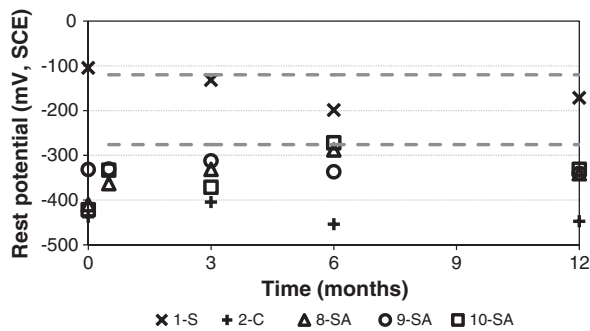


Fig. 12. Evolution of rest potentials for references and treated slabs versus time. 33 days of treatment are not represented in the time scale. (Lines represent ASTM C876 corrosion probabilities [34], which are below 10% when the rest potential is above -120 mV/SCE and above 90% when the rest potential is below -276 mV/SCE.)

strong bands at 220 , 290 , 405 , 630 and 1325 cm^{-1} was not expected in corrosion processes of steel at room temperature, but it can be formed from unstable compounds of iron submitted to high temperature. This is probably the result of the sampling process or local heating due to laser light used for Raman measurement.

The light grey layer, forming the essential part of the corrosion layer, that can be seen in Fig. 15 is a mixture, in various proportions, of at least 4 compounds whose spectra are given in Fig. 17. Fig. 17a is the Raman spectrum of feroxyhite ($\delta\text{-FeOOH}$) that can be distinguished from magnetite by the position of the main Raman band at 650 cm^{-1} instead of 670 cm^{-1} and a large structure at 450 cm^{-1} when magnetite presents two well defined bands at 380 cm^{-1} and 510 cm^{-1} . Fig. 17b is the Raman spectrum of goethite ($\alpha\text{-FeOOH}$). Fig. 17c and d are respectively the Raman spectra of ferrihydrite ($\text{Fe}_2\text{O}_3 \cdot n\text{H}_2\text{O}$) and maghemite ($\gamma\text{-Fe}_2\text{O}_3$). These spectra are closely related by the main band position around 710 – 730 cm^{-1} but the two compounds can be distinguished by the existence of a large band at 1400 cm^{-1} which belongs exclusively to maghemite.

These Raman spectra were selected because they can be considered as pure phases but it should be noticed that almost all the spectra recorded in this part of the corrosion layer were formed of mixtures of two or more of these spectra. Due to the differences in the Raman scattering cross-section of the 4 compounds, it was not possible to analyse in depth the respective contribution of each species.

The external part of the corrosion layer close to concrete and mainly adherent to it is constituted of a mixture of goethite ($\alpha\text{-FeOOH}$) and lepidocrocite ($\gamma\text{-FeOOH}$) depending on the analysis location.

Despite numerous attempts, no difference between treated and reference carbonated concrete was detected in this study. But, depending on the preparation procedure and when water was used

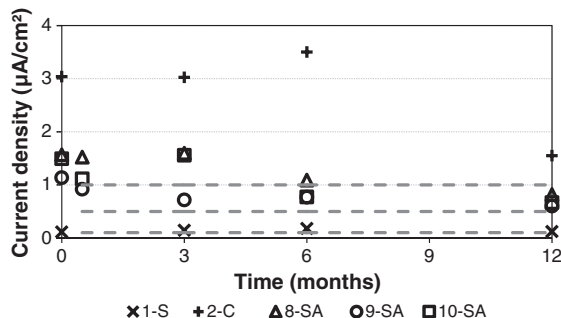


Fig. 13. Evolution of corrosion current densities for references and treated slabs versus time. 33 days of treatment are not represented in the time scale. (Lines represent the four ranges of corrosion levels based on RILEM studies [35], below 0.1 $\mu\text{A}/\text{cm}^2$, the level of corrosion is negligible; from 0.1 to 0.5 $\mu\text{A}/\text{cm}^2$, corrosion is weak; from 0.5 to 1 $\mu\text{A}/\text{cm}^2$, corrosion is moderate and for values higher than 1 $\mu\text{A}/\text{cm}^2$, corrosion is high.)

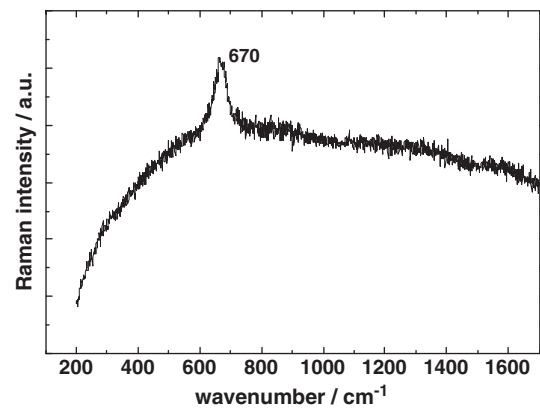


Fig. 14. Raman spectrum recorded on the surface of rebar in sound concrete after 30 months.

in the sampling process, compounds like Green Rusts (iron II, III hydroxide) were detected by Raman spectroscopy. The resulting sampling process gives only stable iron III compounds for the analysis when the difference between a passivated rebar (in sound concrete) and a rebar submitted to a corrosion process (in carbonated concrete) is highlighted by the presence of the corrosion layer. To avoid this sampling process problem, further work was performed on in-situ samples (the results will be presented in a forthcoming paper).

Nevertheless, those results show that, if only magnetite is present (case of sound concrete), the sample is passivated, but the presence of a thin layer of magnetite near the rebar (case observed in carbonated concrete) is not sufficient to prevent further oxidation.

3.2.3.2. Steel/concrete observation using SEM combined to EDS. In the sound concrete reference, SEM examination highlighted the presence of portlandite crystals and the absence of corrosion products on the steel rebar surface (Fig. 18).

The observation of the carbonated samples corroborated the complete carbonation of the cement matrix, portlandite being totally replaced by calcite (Fig. 19a). In addition, a large presence of hexagonal crystals (Fig. 19b) was observed at the steel/concrete interface. EDS analysis (Fig. 19c) showed that iron was the main compound in this area precluding the existence of portlandite. However, the iron oxide type could not be assessed on the basis of the crystals shape as $\text{Fe}(\text{OH})_2$, green rust and feroxyhite belong to the hexagonal system. Yet, presence of iron oxide crystals was indicative of an active corrosion of the rebars embedded in the carbonated concrete. On cross sections, a 10 to 15 μm thick corrosion layer was evidenced before treatment.

After the realisation treatment, no deleterious transformation of the cement matrix was detected. As before treatment, a compact and dense rust layer 10 to 15 μm thick was observed (Fig. 20a).

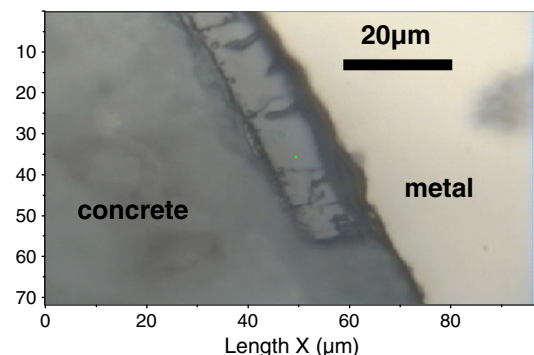


Fig. 15. Optical picture of a cross section of the steel-concrete interface; carbonated concrete after 6 months.

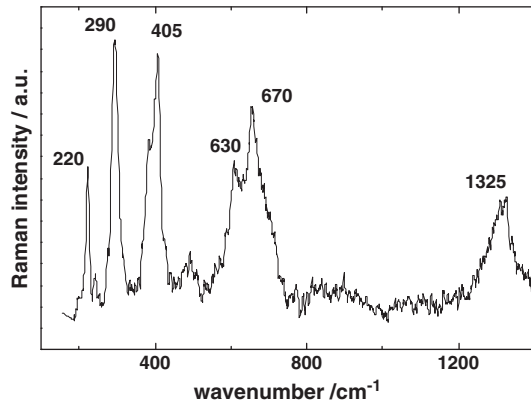


Fig. 16. Raman spectrum recorded near the metal (black sub-layer in Fig. 15).

Nevertheless, EDS analysis evidenced the diffused presence of aluminium and magnesium, probably coming from the sacrificial anode, in the neighbourhood of the rebars (Fig. 20b).

4. Discussion

Concerning the sacrificial anode treatment, comparatively with IC process (1 A/m² of steel), the SA process required 33 days instead of 8–10 days, to reach the recommended total charge of 200 A.h/m² of steel [24]. Elements coming from the anode (aluminium and magnesium) were detected by EDS analysis, but no deleterious neo-compounds were observed. Finally, the 33% total charge discrepancy between slabs 10 and 9 or 8 did not lead to any difference in the electrochemical characterizations.

Concerning the efficiency investigations, one major problem encountered to demonstrate the efficiency of a realkalisation treatment consists in the precise evaluation of the concrete pH. Generally, acid–

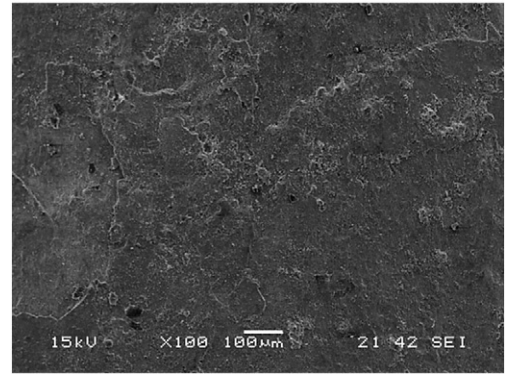


Fig. 18. SEM observations of steel rebar surface in sound concrete reference.

base indicators are used, but they only provide qualitative information, and with time, the colour can become not so obvious [25]. In order to solve this uncertainty, Räsänen's quantitative pH procedure [30] was used and provided interesting results: just after treatment, an increase of the pH around the rebars (from 9 to 11.5) was highlighted and confirmed one year after treatment (pH around rebars = 10.9).

The alkaline ion penetration was also monitored and a significant sodium concentration increase was noticed just after treatment (by 5 times around the rebars, up to 30 times on the treated surface) and no redistribution was observed 12 months after treatment. This result is consistent with Odden's result [10] for longer periods.

Moreover, if the sodium concentrations measured around the rebars are compared to those obtained on the bottom surface (untreated), and combined with the pH measurements, they are consistent with the mechanisms described in Fig. 1: on the bottom surface, the pH increase (from 9 to 10.4) is only linked to a capillary absorption of the alkaline electrolyte whereas around the rebars, the pH increase of the concrete

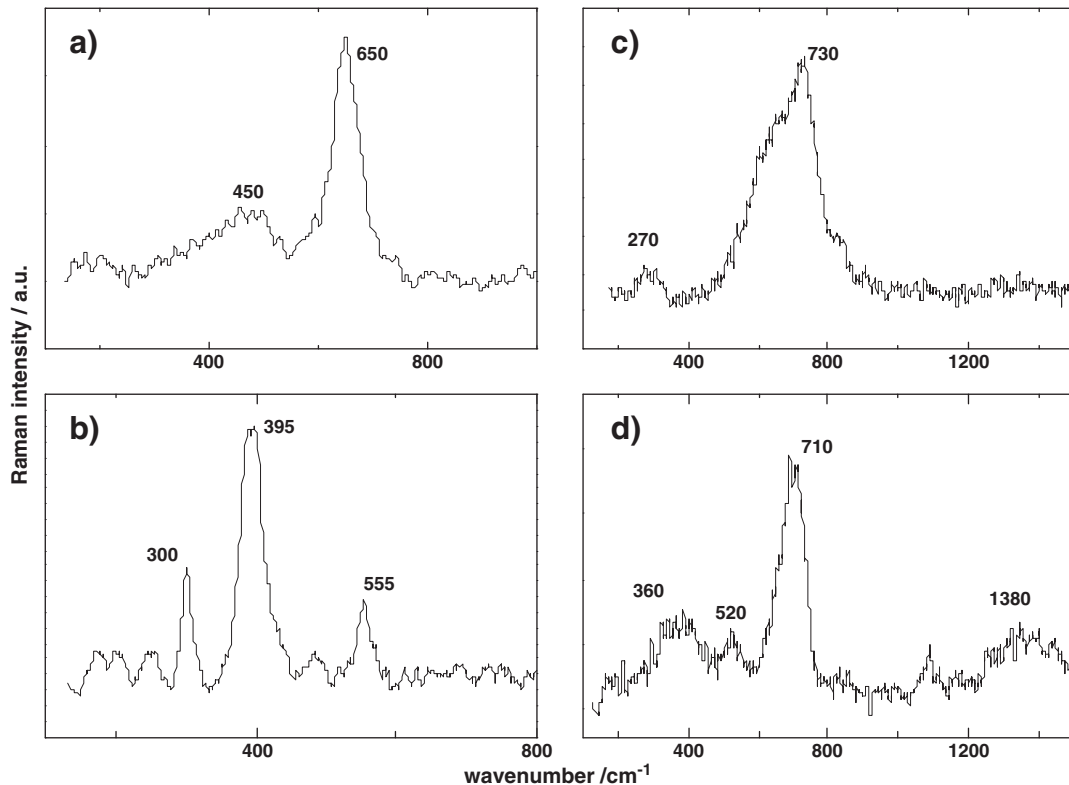


Fig. 17. Raman spectra recorded in different locations in the light grey part of the corrosion layer of Fig. 15.

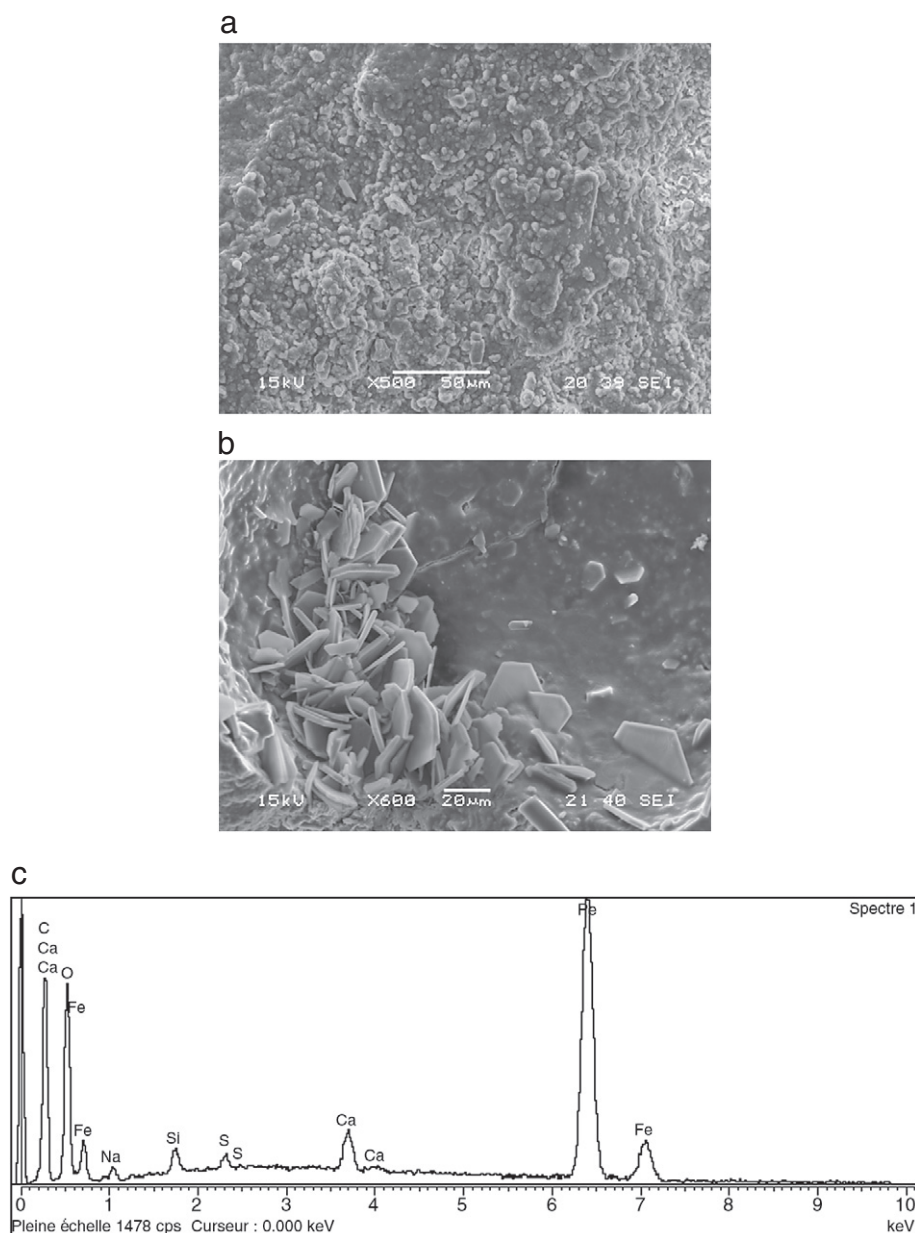


Fig. 19. SEM observations and EDS analysis of the carbonated concrete reference. a) carbonated cement matrix. b) hexagonal crystals at the steel/concrete interface. c) iron oxide crystals, EDS spectrum of b).

(from 8.6 to 11.7) might be attributed to both the penetration of the alkaline electrolyte (absorption and migration) and the formation of hydroxyl ions.

A second delicate point to demonstrate the efficiency of a realkalisation treatment is to highlight a re-passivation of the rebars after treatment. Several authors state that an increase of the pH together with an increase of alkali concentrations are sufficient indicators for re-passivation. Nevertheless, Pollet [20] indicates that “sodium content does not provide direct indication of steel re-passivation nor of the pH value around the rebar”. A complete electrochemical characterisation, not only using half-cell potential measurements (that only gives an idea of the propensity of corrosion), but also using galvanostatic polarisation tests [9,13] or linear polarisation resistance tests [19,21], seems essential. It is well known that electrochemical characterizations are highly influenced by the moisture content of the concrete. A decrease in the moisture content will affect the electrochemical potential of the steel (more positive), the corrosion rate (decreased) and chemical composition of the concrete pore solution (increased ionic concentration).

Therefore, in this study, in order to provide reliable data on electrochemical characterizations of rebars embedded in concrete, not only potential values were monitored but also linear resistance polarisation measurements and electrochemical impedance spectroscopy. This latter technique was used to follow the evolution of the concrete and electrolyte resistance, R_e , before and after treatment versus time (Fig. 21).

Before treatment (time equal to zero), the slabs being all stored in a laboratory at 22 °C and 60%RH, the resistance of the sound concrete slab (1790 ohm) is lower than the ones of the carbonated concrete slabs because carbonation tends to decrease the porosity of the concrete. Moreover, although the concrete slabs were identically fabricated and aged by carbonation, their resistances (mean value = 3335 ohm) show a certain dispersion (standard deviation = 1031 ohm) as concrete is always a heterogeneous material. After 33 days of realkalisation using sacrificial anode, the moisture content of the treated concrete slabs is obviously increased as they have had on their top cover a cellulose pad impregnated with an alkaline solution (which is kept wet daily): therefore the rather dried (60%RH) concrete absorbs the alkaline aqueous

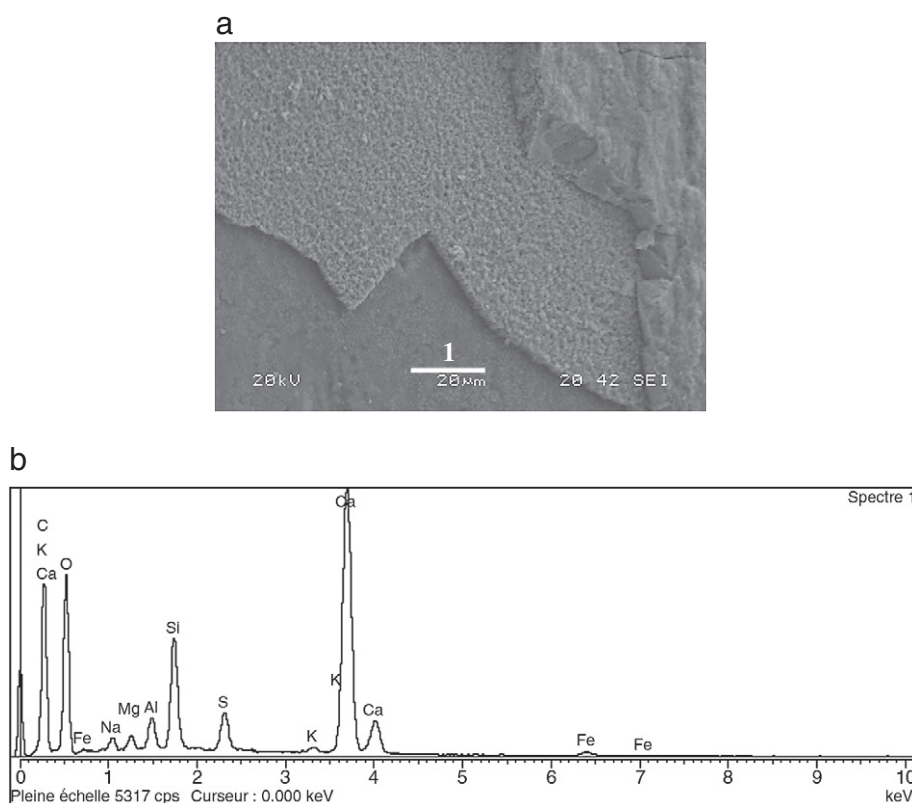


Fig. 20. SEM observation and EDS analysis of the steel–concrete interface of a realkalised slab, 6 months after treatment (11-SA). a) 10 to 15 µm dense oxide layer at the steel–concrete interface ($G = \times 950$). b) Probably treatment-induced diffuse presence of aluminium, magnesium and sodium, in the cement matrix in the neighbourhood of the rebar.

solution and also due to the electrical field the ionic species migrate in the concrete (anions (OH^-) from rebar to top cover and alkaline cations from top cover to rebar). All these mechanisms lead to a drastic change of the concrete around the rebars (moisture as well as composition) which is confirmed by a significant decrease of R_e 15 days after treatment (Fig. 21). Then, the concrete slabs stored in the same laboratory progressively dry (3, 6 and 12 months) and an equilibrium of concrete composition may occur: R_e increases continuously and 12 months after treatment reaches more or less the initial values.

These results show that it is extremely important, for carbonated concrete, to consider the ohmic drop (R_e value) which reflects not only the wetting/drying issue but also the concrete composition changes before calculating the corrosion current density. Finally, although the corrosion current densities cannot be considered as absolute values, they are nevertheless repeatable and comparable.

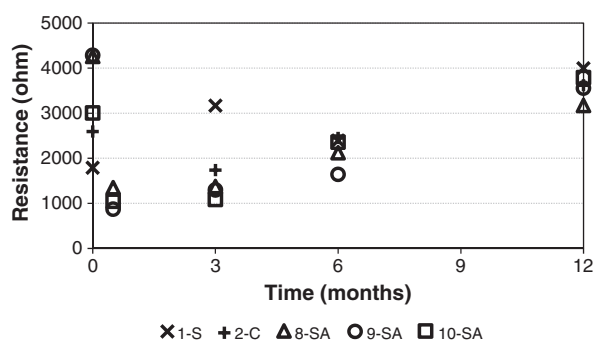


Fig. 21. Evolution of the resistance of the concrete and the electrolyte (R_e) from electrochemical impedance spectroscopy for references and treated slabs versus time. 33 days of treatment are not represented in the time scale.

If some authors consider that a concrete pH value above 10.3 may be sufficient to repassivate steel rebars [18], based on the combined analytical and electrochemical characterisations performed in this study, it seems that a pH of around 11 yields a slowdown of the corrosion rate, but not a repassivation (as the corrosion behaviour of sound concrete is not recovered). Considering this issue, micro-Raman observations can lead to interesting results. This technique provides information on the iron oxide nature and is thus very useful to detect active or stable species after carbonation as well as after the realkalisation treatment. Unfortunately, from the first results of this study, the sample preparation introduces an important source of disturbance in the accurate determination of the oxide species. An in-situ analysis is clearly necessary and therefore, new designed specimens and a new observation electrochemical cell were developed.

Finally, in order to explore realkalisation long term durability, the slabs prepared in this study were submitted to natural ageing and a complementary set of electrochemical and analytical characterization was performed (results will be presented in a forthcoming paper).

5. Conclusions

From this study, the following conclusions can be drawn:

Realkalisation using sacrificial anodes can fulfil the criteria given in the European specification for realkalisation based on impressed current.

The efficiency of the tested realkalisation treatment was demonstrated by a pH increase of the concrete around the rebars (qualitative and quantitative pH tests) together with an enrichment of alkaline into the concrete (alkaline concentration profiles). Moreover, this alkalinity increase was durable at least a year after treatment.

Realkalised concrete showed a slowdown of the steel rebar corrosion activity up to 12 months after treatment, (rest potentials increased and corrosion current densities decreased).

The realkalisation treatment did not induce any deleterious impact on the cement matrix.

Repassivation was not demonstrated by the electrochemical characterizations, as the corrosion behaviour of the sound concrete was never recovered. Neither was repassivation clearly established by the micro Raman experiments, probably because of the sample preparation.

From the different results, realkalisation treatment was found to be effective in reducing the corrosion activity at least during 12 months.

To conclude, although repassivation of the steel rebars could not be demonstrated, a slowdown of the corrosion process was observed, which may be interesting to extend the service life of carbonated structures, by realkalisation.

Acknowledgements

The authors wish to thank the French Ministry responsible for Ecology, Energy, Sustainable Development and Regional Planning, the Ministry of Higher Education and Research and the Ministry of Culture for their financial support. Thanks also to the Freyssinet Company for their technical contribution with the sacrificial anode realkalisation.

References

- [1] J.P. Broomfield, *Corrosion of Steel in Concrete – Understanding, Investigation and Repair*, E&FN SPN, London, 1997.
- [2] A. Raharinaivo, G. Arliguie, T. Chaussadent, G. Grimaldi, V. Pollet, G. Tache, La corrosion et la protection des aciers dans le béton, Presses de l'école nationale des Ponts et Chaussées, Paris, 1998.
- [3] L. Bertolini, B. Elsener, P. Pedeferrri, R. Polder, *Corrosion of Steel in Concrete: Prevention, Diagnosis, Repair*, Wiley, Weinheim, 2004.
- [4] M. Raupach, Concrete repair according to the new European standard EN 1504, International Conference Repair, Rehabilitation and Retrofitting, Cape Town, South Africa, 2005.
- [5] G.P. Tilly, J. Jacobs, CONREPNET – Concrete Repairs – Performance in Service and Current Practice, IHS BRE Press, United Kingdom, 2007.
- [6] Noteby, Norwegian Patent Application N° 875438, 1987.
- [7] D. Pocock, Chloride extraction and realkalisation – six years on, *Corrosion and Protection of Reinforced Concrete*, Dubai, 1994.
- [8] J. Mietz, Electrochemical rehabilitation methods for reinforced concrete structures – a state of the art report, EFC N°24, IOM Communications Ltd, London, 1998.
- [9] J. Mietz, Electrochemical realkalisation for rehabilitation of reinforced concrete structures, *Mater. Corros.* 46 (1995) 527–533.
- [10] L. Odden, The repassivating effect of electro-chemical realkalisation and chloride extraction, in: S.A. Press (Ed.), *Proceedings of International Conference on Corrosion and Corrosion Protection of Steel in Concrete*, Sheffield, United Kingdom, 1994, pp. 1473–1488.
- [11] J.S. Mattila, M.J. Pentti, T.A. Raiski, Durability of electrochemically realkalised concrete, *Corrosion of Reinforcement in Concrete Construction*, Cambridge, 1996.
- [12] T.K.H. Al-Kadhimi, P.F.G. Banfill, S.G. Millard, J.H. Bungey, An experimental investigation into the effects of electrochemical re-alkalisation on concrete, in: C.L. Page, P.B. Bamforth, J.W. Figg (Eds.), *Corrosion of Reinforcement in Concrete Construction*, Sci, Cambridge, 1996.
- [13] G. Sergi, J. Walker, C.L. Page, Mechanism and criteria for the realkalisation of concrete, *Corrosion of Reinforcement in Concrete Construction*, Cambridge, 1996.
- [14] P.F.G. Banfill, Re-alkalisation of carbonated concrete – effect on concrete properties, *Constr. Build. Mater.* 11 (1997) 255–258.
- [15] A.W.M. Van Den Hondel, R. Polder, Laboratory investigation of electrochemical realkalisation of reinforced concrete, European Corrosion Congress, Utrecht, Netherlands, 1998.
- [16] P.F.G. Banfill, T.K.H. Al-Kadhimi, The effect of re-alkalisation and chloride removal on alkali-silica expansion in concrete, European Corrosion Congress, Utrecht, The Netherlands, 1998.
- [17] B. Elsener, L. Zimmermann, D. Burchler, H. Böhni, Repair of reinforced concrete structures by electrochemical techniques – field experience, in: J. Mietz, B. Elsener, R. Polder (Eds.), *European Federation of Corrosion Publications, IOM n°25 communications Ltd*, London, 1998.
- [18] C. Andrade, M. Castellote, J. Sarria, C. Alonso, Evolution of pore solution chemistry, electro-osmosis and rebar corrosion rate induced by realkalisation, *Mater. Struct.* 32 (1999) 427–436.
- [19] J.A. Gonzalez, A. Cobo, M.N. Gonzalez, E. Otero, On the effectiveness of realkalisation as a rehabilitation method for corroded reinforced structures, *Mater. Corros.* 51 (2000) 97–103.
- [20] V. Pollet, Specific information of realkalisation (RE), in: C.A.R. Cigna, U. Nürnberger, R. Polder, R. Weydert, E. Seitz (Eds.), *Corrosion of Steel in Reinforced Concrete Structures, COST 521*, European Commission, Luxembourg, 2003, pp. 141–145.
- [21] W. Yeih, J.J. Chang, A study on the efficiency of electrochemical realkalisation of carbonated concrete, *Constr. Build. Mater.* 19 (2005) 516–524.
- [22] E. Cailleux, E. Marie-Victoire, A. Texier, G. Marchese, Experimental investigations of realkalisation treatments used for restoration of historical monument made of reinforced concrete, International Conference on Concrete Solutions, Saint-Malo, France, 2003.
- [23] L. Bertolini, M. Carsana, E. Redaelli, Conservation of historical reinforced concrete structures damaged by carbonation induced corrosion by means of electrochemical realkalisation, *J. Cult. Herit.* 9 (2008) 376–385.
- [24] FD CEN-TS 14038–1, electrochemical realkalisation and chloride extraction treatments for reinforced concrete part 1: realkalisation, AFNOR, 2005.
- [25] V. Pollet, R. Guerin, C. Tourneur, H. Mahouche, A. Raharinaivo, Concrete realkalisation using sacrificial anode, European Corrosion Congress, Trondheim, Norway, 1997.
- [26] A. Raharinaivo, J.C. Lenglet, C. Tourneur, H. Mahouche, V. Pollet, Chloride removal and realkalisation of concrete using sacrificial anode, International Conference on Corrosion and Rehabilitation of Reinforced Concrete Structures, Orlando, USA, 1998.
- [27] E. Cailleux, E. Marie-Victoire, Influence of the concrete composition on the efficiency and the durability of realkalisation treatment, International Conference on Concrete Solutions, Saint-Malo, France, 2006.
- [28] Y. Tong, Electrochemical realkalisation treatment for the carbonated reinforced concrete repair in, Université Pierre et Marie Curie, Thesis, Paris 6, France, 2009.
- [29] G. Villain, D. Cochet, G. Olivier, M. Thiery, Vers un mode opératoire performant et discriminant de carbonatation accélérée des bétons pour ouvrages d'art, *BLPC 267* (2007) 63–78.
- [30] V. Räsänen, V. Penttala, The pH measurement of concrete and smoothing mortar using a concrete powder suspension, *Cem. Concr. Res.* 34 (2004) 813–820.
- [31] I. Martinez, C. Andrade, N. Rebolledo, V. Bouteiller, E. Marie-Victoire, G. Olivier, Corrosion characterization of reinforced concrete slabs with different devices, *J. Sci. Eng. Cor.* 64 (2008) 107–123.
- [32] F. Wenger, Etude de la corrosion de l'acier doux dans le béton par des méthodes électrochimiques, in, Université Paris Sud, Doctoral Thesis, Orsay, France, 1986.
- [33] J.R. Scully, Polarization resistance method for determination of instantaneous corrosion rates, *Corros.* 56 (2000) 199–217.
- [34] P. Longuet, L. Burglen, A. Zelwer, La phase liquide du ciment hydrate, *Rev. Matér.* 676 (1973) 35–41.
- [35] A.A. Sagüés, E.I. Moreno, C. Andrade, Evolution of pH during in-situ leaching in small concrete cavities, *Cem. Concr. Res.* 27 (1997) 1747–1759.
- [36] L. Li, J. Nam, W.H. Hartt, Ex situ leaching measurement of concrete alkalinity, *Cem. Concr. Res.* 35 (2005) 277–283.
- [37] C 876-91, Standard test method for half-cell potentials of uncoated reinforcing steel in concrete, ASTM, 1999.
- [38] C. Andrade, C. Alonso, Test methods for on-site corrosion rate measurement of steel reinforcement in concrete by means of the polarization resistance method, *Mater. Struct.* 37 (2004) 623–643.
- [39] T.D. Marcotte, C.M. Hansson, The influence of silica fume on the corrosion resistance of steel in high performance concrete exposed to simulated sea water, *J. Mater. Sci.* 38 (2003) 4765–4776.